ARTICLE

Synthesis of Amino-Functionalized Polyester via Ring-Opening Alternating Copolymerization of Glycidylamines with Cyclic Anhydrides

Received 00th January 20xx,
Accepted 00th January 20xx

DOI: 10.1039/x0xx00000x

Ryota Suzuki,[a] Tianle Gao,[a] Ayaka Sumi,[b] Takuya Yamamoto,[b] Kenji Tajima,[b] Feng Li,[b] Takuya Isono *[,b] and Toshifumi Satoh*[,b,c]

Amino-functionalized polyesters (APEs) are a remarkable class of polymeric materials with a wide range of applications, e.g. as antibacterial materials, gene delivery carriers, and biodegradable plastics. However, the current APE synthetic pathway poses significant challenges in terms of structural diversity and control over polymerization. In this study, we explored the ring-opening alternating copolymerization (ROAC) of glycidylamines with cyclic anhydrides as a novel method of synthesizing APEs. The ROAC of *N*,*N*-dibenzylglycidylamine (DBGA) and phthalic anhydride (PA) successfully proceeded to yield the corresponding alternating copolymer poly(PA-*alt*-DBGA), with a typical molecular weight and dispersity of 5450–21 000 g mol^{-1} and 1.10–1.62, respectively, using an alkali metal carboxylate or a phosphazene base as a catalyst. Kinetic and chain extension studies of the *t*-BuP_1-catalyzed ROAC revealed its controlled/living nature, which enabled us to produce block copolyesters comprising APE and polyethylene glycol and install a functional end-group using a functionalized alcohol initiator. In addition, we prepared several poly(cyclic anhydride-*alt*-glycidylamine)s with different main-chain structures using different monomers. Based on the advantages of chain-growth polymerization and the wide monomer scope, the developed ROAC system may accelerate the investigation of novel APEs for use in different applications.

Introduction

Amino-functionalized polymers, which contain amino groups on their main- or side-chains, are critical functionalized polymers because of their widespread application as surface modifiers,[1] adhesives,[2–4] heavy metal-ion scavengers,[5] antibacterial materials,[6,7] and gene delivery carriers.[8,9] Poly(ethylene imine) is the most well-known amino-functionalized polymer, and numerous other types, including polystyrenes,[10,11] polyethers,[12–17] polyesters,[8,9,18–20] poly(ester amide),[21] and poly(acryl amide),[22–24] have been reported. Of these, amino-functionalized polyesters (APEs) garner particular attention because of their intriguing properties and functionalities derived from their amino groups, in addition to their inherent degradabilities via chemical and biological processes. APEs have been used as gene delivery carriers, antibacterial coatings, and biodegradable materials. However, owing to synthetic challenges and the potential incompatibilities of basic amines and esters, the methods of synthesizing APEs are limited.[25]

Existing APE syntheses can be classified into two categories based on the polymerization mechanism: (a) chain-growth polymerization and (b) step-growth polymerization. The former can be further classified into three categories: the (a-1) ring-opening polymerization (ROP) of lactone monomers with unprotected tertiary amine functionalities,[9] (a-2) ROP of protected amine monomers, followed by deprotection,[20,26–31] and (a-3) ROP of functionalized monomers, followed by post-modification (**Figure 1**).[32–34] The example of (a-1) is the ROP of tertiary amine-bearing valerolactone.[9] Unlike tertiary amine, primary and secondary amines can initiate ROP of cyclic esters, so that the protection and deprotection steps are necessary for the synthesis of APEs with primary and secondary amines. As for example of the (a-2) approach, Tao and Wang et al. performed the living ROP of *O*-carboxyanhydride monomer derived from bio-sourced lysine under mild conditions, and the subsequent deprotection yielded a polyester with primary amines on the side chains.[30] Nottelet et al. also reported an APE synthesis based on the ROP of protected amine-containing lactone, followed by deprotection, where the copolymerization of benzyloxycarbonyl-protected 5-amino-*δ*-valerolactone with ε-caprolactone successfully produced APEs with amine contents of 10–100%.[35] Waymouth et al. succeeded in synthesizing polyesters with amino groups in their main chains via the organo-catalytic ROP of *N*-acyl-substituted morpholin-2-ones, followed by deprotection.[31] As a third approach, Cheng et al. synthesized APEs by ROP of alkyne subsutited *O*-carboxyanhydride, followed by thiol-yne click reaction (a-3).[33] The advantages of these three methods lie in the precise control

[a] *Graduate School of Chemical Sciences and Engineering, Hokkaido University, Sapporo 060-8628, Japan*
[b] *Division of Applied Chemistry, Faculty of Engineering, Hokkaido University, Sapporo 060-8628, Japan*
[c] *List Sustainable Digital Transformation Catalyst Collaboration Research Platform (ICReDD List-PF), Institute for Chemical Reaction Design and Discovery, Hokkaido University, Sapporo 001-0021, Japan*
E-mail: isono.t@eng.hokudai.ac.jp; satoh@eng.hokudai.ac.jp
† Electronic Supplementary Information (ESI) available. See DOI: 10.1039/x0xx00000x

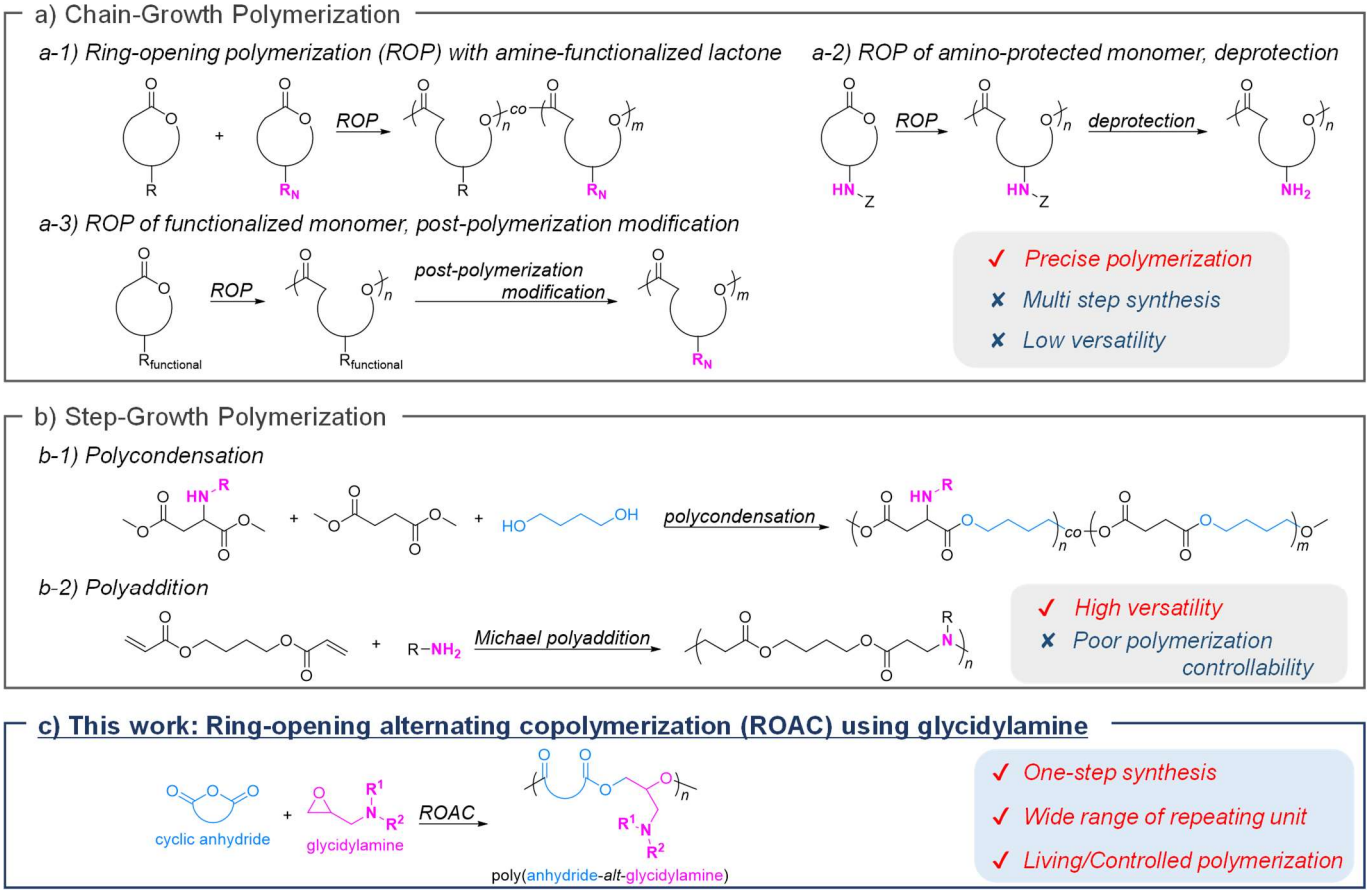

Figure 1. Methods of synthesizing APEs: a) Chain-growth polymerization, b) step-growth polymerization, and c) ring-opening alternating polymerization using glycidylamine.

over the molecular weight, monomer sequence, and chain ends, based on the living characteristics of ROP. However, a major drawback of the ROP approach is the limited versatility in the design of applicable monomers, which renders the production of various APEs with different main- and side-chain structures challenging. Moreover, most of these monomers require multistep syntheses and deprotection after ROP.

Another major approach used in synthesizing APEs is step-growth polymerization involving polycondensation (b-1) and polyaddition (b-2), as shown in **Figure 1**.[36–40] Wu et al. synthesized an APE via the polycondensation of diols and diesters with amino-substituted diesters.[36] Michael addition polymerization was also used in APE synthesis, e.g. Anderson et al. reported the Michael polyaddition of bis(acrylate esters) with primary or secondary amines to yield APEs.[37,38] APEs can be synthesized by converting unsaturated polyesters via aza- or thiol-Michael reactions, utilizing primary amines and amino thiols, respectively.[39,40] The advantage of step-growth polymerization lies in the generation of the polymer main chain using two different types of monomers (e.g. diol and dicarboxylic acid), enabling the facile syntheses of polyesters with diverse main-chain structures. However, the challenge in controlling polymerization, e.g. the molecular weight, dispersity, chain-end structures, and monomer sequence, is a major drawback of step-growth polymerization. Therefore, developing a simple, versatile method of synthesizing APEs to explore the structure-property relationships and expand the range of applications is still challenging.

Herein, we propose the use of ring-opening alternating copolymerization (ROAC) in the efficient syntheses of APEs. The ROAC of cyclic anhydrides and epoxides recently attracted intense attention as a novel approach for use in producing functional polyesters. The remarkable advantages of ROAC lie in the precise control over polymerization based on its controlled/living chain-growth polymerization nature and the structural diversity of the resulting polyesters derived from the two different types of monomers, i.e. ROAC simultaneously combines the advantages of the ROP and step-growth approaches in APE synthesis. A recent report by Wu clearly demonstrates that ROAC can serve as a complementary polymerization process to polycondensation, particularly in the synthesis of high value-added products.[41] Thus, the ROAC of cyclic anhydrides with amino-functionalized epoxides may be an excellent synthetic platform for APEs with diverse main- and side-chain structures, controlled monomer sequences, and desirable chain-end structures.

Glycidylamines are amino-functionalized epoxides that can be readily prepared in a single step using epichlorohydrin and secondary amines. Frey et al. pioneered the ROP of glycidyl amines bearing different side chains, where cesium alkoxide-

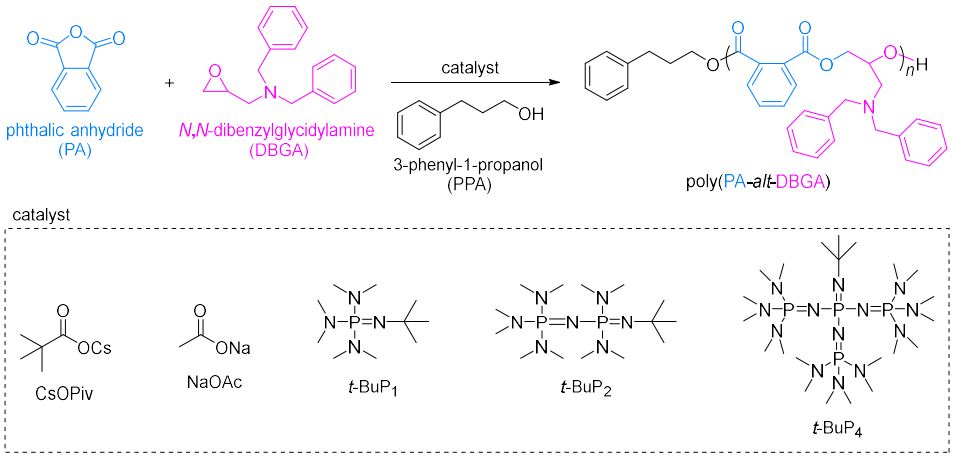

Scheme 1. Ring-opening alternating copolymerization of PA and DBGA.

mediated anionic ROP with an ethylene oxide co-monomer afforded amino-functionalized polyethers.[13,42–44] Additionally, our group reported the homopolymerization of glycidylamines compatibilities of glycidylamines with base-catalyzed ROAC conditions. However, despite the rapid growth in ROAC research, no studies regarding APE synthesis via ROAC have been reported, except for our previous study demonstrating the cesium pivalate (CsOPiv)-catalyzed ROAC of a specific combination of a glycidylamine and cyclic anhydride: *N*,*N*-dibenzylglycidylamine (DBGA) with phthalic anhydride (PA) or trimellitic anhydride to produce linear and hyperbranched APEs.[45]

In this paper, we report a systematic study regarding the ROAC of glycidylamine with cyclic anhydrides to produce diverse APEs. In our previous study, we employed CsOPiv as a catalyst. However, catalyst screening revealed that polymerization control could be further improved using a phosphazene base. Utilizing the optimized conditions, we successfully synthesised APEs with controlled molecular weights based on the initial monomer-to-initiator ratio. APEs with different main and side chains and chain-end structures were synthesized using different glycidylamine and cyclic anhydride monomers, in addition to an alcohol initiator. Moreover, we examined a glycidylamine/non-amino functionalized epoxide/cyclic anhydride ternary monomer system to maximize the accessible molecular design of the APE.

Results & discussion

ROAC of PA and DBGA

To optimize the polymerization conditions for the ROAC of glycidylamines and cyclic anhydrides, we evaluated several base catalysts that have been used in ROAC. The evaluated catalysts include alkali metal carboxylates, such as CsOPiv and sodium acetate (NaOAc),[45–50] and phosphazene bases,[51] such as *t*-BuP_1, *t*-BuP_2, and *t*-BuP_4 (runs 1–5 in **Table 1**). In catalyst screening, DBGA and PA are used as the glycidylamine and cyclic anhydride monomers, respectively (**Scheme 1**).

Initially, we examined ROAC using 3-phenyl-1-propanol (PPA) and CsOPiv as the initiator and catalyst, respectively, at an initial [CsOPiv]/[PPA]$_0$/[PA]$_0$/[DBGA]$_0$ ratio of 1/1/25/75 at 80 °C in bulk (run 1 in **Table 1**). After 9 h, ^{1}H nuclear magnetic resonance (NMR) spectroscopy of the reaction mixture reveals a PA conversion (conv.$_{PA}$) of 77%, and the ^{1}H NMR spectrum of the obtained polymer closely matches that of poly(PA-*alt*-DBGA) reported in our previous study (**Figure 2**). The ^{1}H NMR spectrum displays the characteristic signals representing the main (benzene ring of PA (*a*), 7.03–7.75 ppm; –C*H*$_2$CH– (*b*), 4.27–4.72 ppm; –CH$_2$C*H*– (*c*), 5.42–5.68 ppm) and DBGA side chains (–CHC*H*$_2$O– (*d*), 2.69–3.04 ppm; –N(C*H*$_2$C$_6$H$_5$)$_2$ (*e*), 3.44–3.77 ppm; –C$_6$*H*$_5$ (*f*), 7.03–7.75 ppm), in addition to the terminal initiator group (C$_6$H$_5$C*H*$_2$– (*B*), 2.65 ppm; C$_6$H$_5$CH$_2$C*H*$_2$– (*C*),

Table 1. Ring-opening alternating copolymerization of PA and DBGA using different catalysts [a]

run	catalyst	time (h)	conv.$_{PA}$ (%) [b]	$M_{n,theo.}$ (g mol^{-1}) [c]	$M_{n,NMR}$ (g mol^{-1}) [b]	$M_{n,SEC}$ (g mol^{-1}) [d]	$Đ$ [d]
1	CsOPiv	9.0	77	7800	7100	2670	1.62
2	NaOAc	6.5	68	6900	11 700	3380	1.19
3	*t*-BuP_1	2.5	80	6900	8000	3760	1.10
4	*t*-BuP_2	1.5	86	8700	8000	2560	1.20
5	*t*-BuP_4	0.8	88	9000	8300	3330	1.35
6	None	6.5	69	7100	5500	3510	1.18
7 [e]	*t*-BuP_1	5.0	61	12 000	14 300	4130	1.16
8 [f]	*t*-BuP_1	6.0	59	24 000	21 000	4370	1.19

[a] Polymerization conditions: temp., 80 °C; atmosphere, Ar; initiator, PPA; monomers, PA and DBGA; [catalyst]/[PPA]$_0$/[PA]$_0$/[DBGA]$_0$ = 1/1/25/75. [b] Determined via ^{1}H NMR spectroscopy in $CDCl_3$. [c] Calculated via (molecular weight (M.W.) of PPA) + [PA]$_0$/[PPA]$_0$ × conv.$_{PA}$ × (M.W. of PA + M.W. of DBGA). [d] Determined via SEC in dimethylformamide (DMF) containing 0.01 mol L^{-1} LiCl using a polystyrene (PSt.) standard. [e] [*t*-BuP_1]/[PPA]$_0$/[PA]$_0$/[DBGA]$_0$ = 1/1/50/150. [f] [*t*-BuP_1]/[PPA]$_0$/[PA]$_0$/[DBGA]$_0$ = 1/1/100/300.

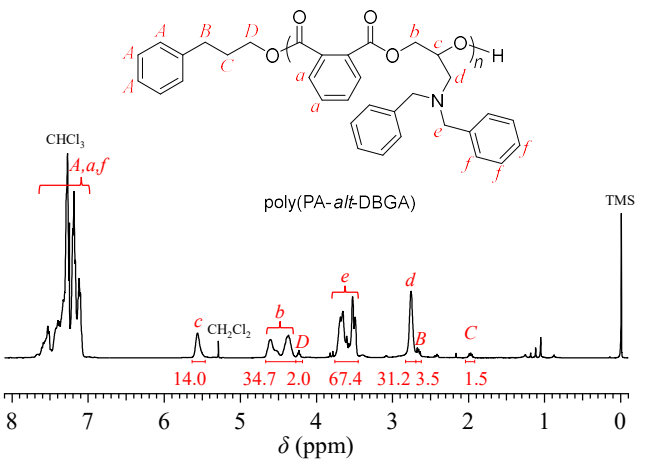

Figure 2. ^{1}H NMR spectrum of poly(PA-*alt*-DBGA) obtained via run 1 in Table 1 ($CDCl_3$, 400 MHz).

1.98 ppm; $C_6H_5CH_2CH_2CH_2$– (*D*), 4.22 ppm). Size exclusion chromatography (SEC) reveals a monomodal size distribution, which is used to calculate the number-average molecular weight ($M_{n,SEC}$) and dispersity (*Đ*) of 2670 g mol^{-1} and 1.62, respectively, based on polystyrene calibration (**Figure S1**). These results confirm the success of the ROAC of the cyclic anhydride and glycidylamine in producing an alternating copolyester with amino-functionalized side chains.

Under similar conditions, ROAC was performed using NaOAc as the catalyst (run 2 in **Table 1**). NaOAc is used as a food additive to ensure a high safety. conv.$_{PA}$ reaches 68% after 6.5 h, affording the desired poly(PA-*alt*-DBGA) with an even narrower *Đ* of 1.19. This suggests that the control over polymerization can be further improved via careful catalyst selection.

To obtain a polymer with a narrower *Đ*, we then examined phosphazene bases as catalysts. Notably, the use of these catalysts leads to higher levels of conv.$_{PA}$ in shorter times compared to those observed using the alkali metal carboxylate catalysts (runs 3–5 in **Table 1**). Furthermore, as the basicity of the phosphazene base increases (*t*-BuP$_1$, pK_{BH^+} = 26.9; *t*-BuP$_2$, pK_{BH^+} = 33.5; *t*-BuP$_4$, pK_{BH^+} = 42.7),[51] the polymerization rate increases. Moreover, the $M_{n,NMR}$ values of the poly(PA-*alt*-DBGA) obtained using the phosphazene bases closely match the theoretical molecular weights ($M_{n,theo.}$). Slight increases in *Đ* are observed when utilizing *t*-BuP$_2$ and *t*-BuP$_4$ (*Đ* = 1.20 and 1.35, respectively), which may be due to side reactions, such as

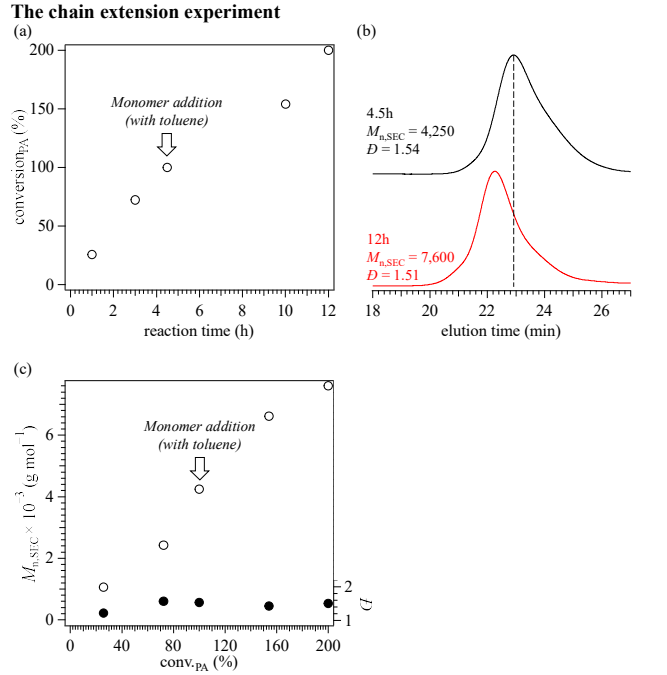

Figure 3. (a) Time to conv. Plot in the first ROAC of PA and DBGA ([*t*-BuP$_1$]/[PPA]$_0$/[PA]$_0$/[DBGA]$_0$ = 1/1/25/75) and following monomer addition ([living poly(PA-*alt*-DBGA chain]$_0$/[PA]$_0$/[DBGA]$_0$ = 1/25/75). (b) SEC curves of poly(PA-*alt*-DBGA) obtained via the first copolymerization (black line; $M_{n,NMR}$ = 7300 g mol^{-1}, $M_{n,SEC}$ = 4250 g mol^{-1}, *Đ* = 1.54) and following chain extension (red line; $M_{n,NMR}$ = 16 800 g mol^{-1}, $M_{n,SEC}$ = 7600 g mol^{-1}, *Đ* = 1.51). (c) Kinetic plots of chain extension experiment.

transesterification, promoted by their exceedingly strong basicities (**Figure S2**). In general, basic and acidic catalysts are indispensable in the ROAC of cyclic anhydrides and epoxides. Remarkably, the ROAC of PA and DBGA proceeds even without a catalyst (run 6 in **Table 1**). As ROAC proceeds via an anionic polymerization mechanism when a basic catalyst is used, the ROAC of DBGA may be catalyzed by its tertiary amine moiety. To evaluate this hypothesis, we examined the ROAC of PA and butylene oxide (BO) in the presence of a large quantity of a tertiary amine (triethylamine; TEA) at an initial [PPA]$_0$/[PA]$_0$/[BO]$_0$/[TEA] ratio of 1/25/75/75 (**Table 2**). Expectedly, ^{1}H NMR spectroscopy reveals a conv.$_{PA}$ of >99% after 6.5 h and the formation of the corresponding alternating copolymer poly(PA-*alt*-BO) (**Figure S3**). Therefore, the tertiary amine moiety of the glycidylamine monomer acts as a catalyst in ROAC. Nevertheless, considering the molecular weight controllability and lowest *Đ*, *t*-BuP$_1$ is the optimal catalyst for use in this ROAC system.

Table 2. ROAC of PA and BO with excess amount of tertiary amine as a catalyst [a]

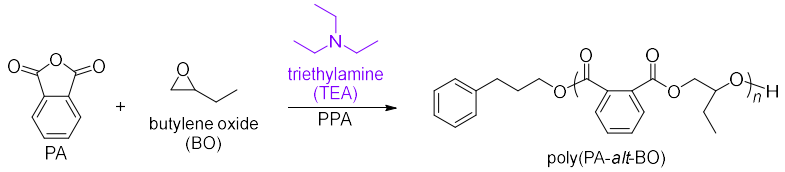

run	monomer	catalyst	[PPA]$_0$/[PA]$_0$/ [BO]$_0$/[TEA]	time (h)	conv.$_{PA}$ (%) [b]	$M_{n,NMR}$ [b]	$M_{n,SEC}$ [c]	*Đ* [c]
1	PA/BO	TEA	1/25/75/75	6.5	>99	5200	1910	1.39

[a] Polymerization conditions: temp., 80 °C; atmosphere, Ar; initiator, PPA; catalyst, TEA; monomer, PA and BO. [b] Determined via ^{1}H NMR in $CDCl_3$. [c] Determined via SEC in DMF containing 0.01 mol L^{-1} LiCl using PSt. standard.

Table 3. ROAC of PA and DBGA using different alcohol initiators [a]

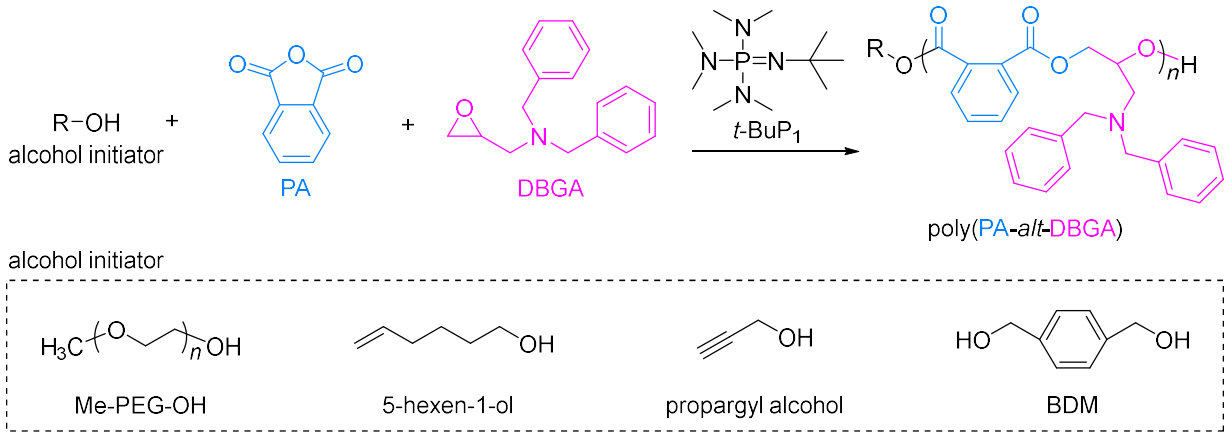

run	initiator	time (h)	conv.$_{PA}$ (%) [b]	$M_{n,theo.}$ (g mol^{-1}) [c]	$M_{n,NMR}$ (g mol^{-1}) [b]	$M_{n,SEC}$ (g mol^{-1}) [d]	$Đ$ [d]
1	Me-PEG-OH	6	69	7300	6700	4830	1.22
2	5-hexen-1-ol	10	67	6800	7200	5240	1.16
3	propargyl alcohol	6	90	9000	9000	5240	1.20
4	BDM	3	79	8000	7900	4150	1.21
5	none	154	66	*N.D.* [e]	*N.D.* [e]	44 500	1.43

[a] Polymerization conditions: temp., 80 °C; atmosphere, Ar; catalyst, *t*-BuP$_1$; monomers, PA and DBGA; [*t*-BuP$_1$]/[initiator]$_0$/[PA]$_0$/[DBGA]$_0$ = 1/1/25/75. [b] Determined via ^{1}H NMR spectroscopy in $CDCl_3$. [c] Calculated using (M.W. of PPA) + [PA]$_0$/[PPA]$_0$ × conv.$_{PA}$ × (M.W. of PA + M.W. of DBGA). [d] Determined via SEC in DMF containing 0.01 mol L^{-1} LiCl using a PSt. standard. [e] Not determined.

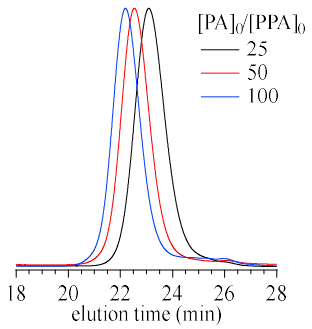

Figure 4. SEC traces of the poly(PA-*alt*-DBGA) polymers with different molecular weights prepared by varying the initial monomer-to-initiator ratio ([PA]$_0$/[PPA]$_0$ = 25, 50, and 100; runs 3, 7, and 8 in Table 1, respectively).

To investigate the microstructure of the poly(PA-*alt*-DBGA) obtained by the optimized condition in more detail, we employed ^{13}C NMR and matrix-assisted laser desorption ionization-time-of-flight (MALDI-TOF) mass spectrometry. In a typical ROAC of cyclic anhydrides and epoxides, ROP of epoxides, leading to polyether homopolymer formation or ether linkage formation in the resulting copolymer, can occur as a side reaction.[52,53] However, as shown in **Figure S4**, the MALDI-TOF mass spectrum of the product obtained from *t*-BuP$_1$-catalyzed ROAC exhibited two series of peaks with regular intervals of 400.8 Da corresponding to the unit molecular weight of the alternating copolymer (401.2 Da), confirming the perfectly alternating monomer sequence as well as no ether linkage. To further verify the absence of poly(glycidylamine) homopolymer and ether linkage, we compared the ^{13}C NMR spectrum of the obtained poly(PA-*alt*-DBGA) with poly(DBGA) homopolymer. According to previous reports, a signal originating from the tertiary carbon of the poly(DBGA) main chain appears at 79 ppm,[13,17] which can be used as the signature for the unwanted ROP of DBGA. However, the ^{13}C NMR spectrum of poly(PA-*alt*-DBGA) (run 3 in **Table 1**) showed no signal around 79 ppm (**Figure S5**). Based on these results, we concluded that the *t*-BuP$_1$-catalyzed polymerization solely proceeded by the alternating copolymerization mechanism, without continuous insertion of DBGA.

After determining the optimized conditions, we investigated the living nature of the copolymerization via a monomer addition study (**Figure 3**). The ROAC of PA and DBGA was perfomed under the same conditions as those of run 3 in **Table 1**. conv.$_{PA}$ increases with reaction time and reaches >99% at 4.5 h (**Figure 3**(a)). After confirming the complete conversion of PA, additional PA and DBGA (25 and 75 equiv. with respect to PPA, respectively, dissolved in a small amount of toluene) were added to the reaction mixture. Expectedly, conv.$_{PA}$ increases further, even after monomer addition. Critically, upon monomer addition, the SEC elution peak shifts to a higher molecular weight region without broadening, indicating chain extension from the end of the living polymer chain (**Figure 3**(b)). Moreover, $M_{n,SEC}$ increases with increasing conv.$_{PA}$, whereas the $Đ$ of approximately 1.5 is maintained (**Figure 3**(c)). These results confirm the controlled/living nature of this ROAC system.

Exploiting its living nature, we attempted to synthesize poly(PA-*alt*-DBGA) with different molecular weights by varying the [monomer]$_0$/[initiator]$_0$ ratio from 25 to 100 (runs 7–8 in **Table 1**). The polymerizations proceed quantitatively, and the SEC traces of the obtained products shift to the high molecular weight region as [monomer]$_0$/[initiator]$_0$ increases while narrow $Đ$ values are maintained (1.10–1.19, **Figure 4**). In

addition, the $M_{n,NMR}$ values are fairly consistent with the $M_{n,theo}$ values, with the $M_{n,NMR}$ values of 8000, 14 300, and 21 000 g mol^{-1} corresponding to the $M_{n,theo}$ values of 6900, 12 000, and 24 000 g mol^{-1}, respectively.

ROAC of PA and DBGA with functionalized initiators

To demonstrate the intrinsic advantages of this strategy, several functionalized initiators were used to synthesise poly(PA-*alt*-DBGA) polymers with various chain-end functionalities (**Table 3**). First, we employed poly(ethylene glycol) with a hydroxyl group at one end (Me-PEG-OH; $M_{n,NMR}$ = 400 g mol^{-1}; $M_{n,SEC}$ = 1070 g mol^{-1}) as a macroinitiator in synthesizing APE-based block copolymers. Even if we use Me-PEG-OH instead of PPA, the ROAC of PA and DBGA ([t-BuP$_1$]/[Me-PEG-OH]$_0$/[PA]$_0$/[DBGA]$_0$ = 1/1/25/75) proceeds smoothly, affording PEG-*b*-poly(PA-*alt*-DBGA) with a narrow dispersity (*Đ* = 1.22; run 1 in **Table 3**). A clear shift in the SEC elution peak toward the higher molecular weight region compared to that of the Me-PEG-OH macroinitiator suggests chain extension from the hydroxyl group of the macroinitiator (**Figure S6**). The ^{1}H NMR spectrum of the product displays the proton signals representing the terminal methoxy (–OC*H*$_3$, (*A*), 3.4 ppm) and main chain methylene groups of the PEG chain (–C*H*$_2$C*H*$_2$O– (*B*), 3.5–3.7 ppm; (*C*), 4.3 ppm), in addition to the proton signals representing the poly(PA-*alt*-DBGA) backbone (**Figure S7**). Such PEG-containing APE block copolymers may be applied in the biomedical field, e.g. as a pH-responsive nanocarrier for drug delivery systems (DDS).[54] Subsequently, to synthesize end-functionalized poly(PA-*alt*-DBGA)s, alcohols with alkene and alkyne functional groups, i.e. 5-hexen-1-ol and propargyl alcohol, were used as initiators (runs 2 and 3 in **Table 3**). The ^{1}H NMR spectra of the obtained products display the characteristic signals representing the alkene (–CH=C*H*$_2$, (*A*), 4.9 ppm; –C*H*=CH$_2$, (*B*), 5.8 ppm) and alkyne protons (–C≡C*H*, (*A*), 3.1 ppm, **Figures S8** and **S10**). The SEC traces of the alkene- and alkyne-functionalized poly(PA-*alt*-DBGA) polymers display monomodal elution peaks, suggesting the well-controlled natures of the polymerizations (*Đ* = 1.16–1.20; **Figures S9–S10**). These reactive end groups can be used for further functionalization. Furthermore, the diol initiator 1,4-benzenedimethanol (BDM) successfully provides the desired product (run 4 in **Table 3** and **Figure S11**). These results confirm the advantages of the ROAC approach in synthesizing functionalized, well-defined APEs.

To determine the role of the alcohol initiator in the ROAC system, we conducted the ROAC of PA and DBGA without an initiator. Initially, it was expected that polymerization would not occur. However, polymerization proceeds slowly and a conv.$_{PA}$ of 66% is reached after 154 h, affording a high-molecular-weight poly(PA-*alt*-DBGA) ($M_{n,SEC}$ = 44 500 g mol^{-1}, *Đ* = 1.43; run 5 in **Table 3** and **Figure S12**). This suggests that trace amounts of protic impurities, such as H_2O, a diol derived from DBGA, and a dicarboxylic acid derived from PA, act as initiators.

Monomer scope

The monomer scope of the ROAC system was then investigated using four cyclic anhydrides and three glycidylamines (**Scheme 2** and **Table 4**). First, ROACs with PA were conducted using *N*-benzyl-*N*-methylglycidylamine (BMGA) and *N*,*N*-diallylglycidylamine (DAGA) as glycidylamine monomers (runs 1 and 2 in **Table 4**). The ROAC of PA and BMGA successfully produces the desired polymer poly(PA-*alt*-BMGA), as confirmed

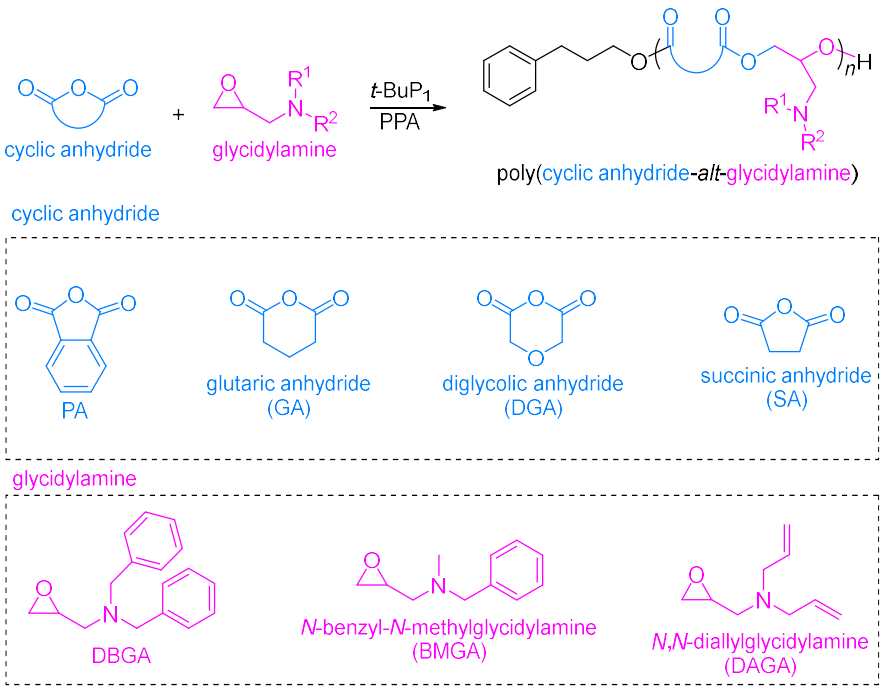

Scheme 2. ROAC of cyclic anhydride and glycidylamine.

Table 4. ROAC of various cyclic anhydrides and glycidylamines using *t*-BuP$_1$ as the catalyst [a]

run	M1	M2	time (h)	conv.$_{M1}$ (%) [b]	$M_{n,theo.}$ (g mol^{-1}) [c]	$M_{n,NMR}$ (g mol^{-1}) [b]	$M_{n,SEC}$ (g mol^{-1}) [d]	$Đ$ [d]	T_g (°C) [e]
1	PA	BMGA	2.5	74	6100	4600	2350	1.41	30.8
2	PA	DAGA	1.0	>99	7700	5300	2480	1.30	23.4
3	GA	DBGA	7.0	76	9300	2000	4390	1.50	8.8
4	DGA	DBGA	3.0	74	9400	N.D. [f]	5000	1.86	20.3
5	SA	DBGA	7.0	67	9000	4900	6800	2.22	23.5

[a] Polymerization conditions: temp., 80 °C; atmosphere, Ar; initiator, PPA; catalyst, *t*-BuP$_1$; [*t*-BuP$_1$]/[PPA]$_0$/[cyclic anhydride]$_0$/[glycidylamine]$_0$ = 1/1/25/75. [b] Determined via ^{1}H NMR spectroscopy in $CDCl_3$. [c] Calculated using (M.W. of PPA) + [cyclic anhydride]$_0$/[PPA]$_0$ × conv.$_{cyclic\ anhydride}$ × (M.W. of cyclic anhydride + M.W. of glycidylamine). [d] Determined via SEC in DMF containing 0.01 mol L^{-1} LiCl using a PSt. standard. [e] Measured using DSC. [f] Not determined.

via ^{1}H NMR spectroscopy and SEC (**Figure S13**). The ^{1}H NMR spectrum displays the characteristic signals representing the methyl (2.1–2.5 ppm (*g*)) and benzyl (–C*H*$_2$C$_6$H$_5$, (*e*), 3.4–3.6 ppm; –C$_6$*H*$_5$, (*f*), 7.1–7.3 ppm) moieties of the BMGA units. In copolymerizing PA and DAGA, the allyl groups isomerize to propenyl groups during the polymerization (–C*H*=CHCH$_3$, (*h*), 5.8 ppm; –CH=C*H*CH$_3$, (*i*), 4.3 ppm; –CH=CHC*H*$_3$, (*j*, *k*), 1.4 and 1.6 ppm), as confirmed by the ^{1}H NMR spectrum (**Figure S14**). Such isomerization in the anionic ROP of DAGA under harsh conditions has been reported by Frey *et al*.[13]

We evaluated the ROAC of DBGA with different cyclic anhydrides, including glutaric anhydride (GA), diglycolic anhydride (DGA), and succinic anhydride (SA) (runs 3–5 in **Table 4**). Although the polymerization rate varies depending on the cyclic anhydride used, the ROACs proceed with levels of cyclic anhydride conversion of >65%, affording the desired products: poly(GA-*alt*-DBGA), poly(DGA-*alt*-DBGA), and poly(SA-*alt*-DBGA) (**Figures S15–S17**). The SEC trace of poly(SA-*alt*-DBGA) displays a bimodal elution peak, where the higher-molecular-weight byproduct may be due to the polymer chain that grows bidirectionally from a trace amount of succinic acid. In addition to the cyclic anhydrides evaluated, we already reported the ROAC of trimellitic anhydride and DBGA to generate a hyperbranched APE in our previous study.[45] It is notable that for all the obtained copolyesters, no evidence of the ether linkage formation via ROP of glycidylamine was detected from their ^{13}C NMR spectra (**Figure S18**–**S22**). These results collectively confirm the broad monomer scope of the ROAC system.

The thermal properties of the APEs with different main-chain structures were evaluated using thermogravimetric analysis (TGA) and differential scanning calorimetry (DSC). Based on TGA, the 5% mass loss temperatures ($T_{d,5\%}$) are in the range 220–305 °C, indicating sufficient thermal stabilities (**Figure S23**). The DSC thermograms of all APEs display baseline shifts corresponding to the glass transition temperatures (T_g), whereas no other transitions, such as melting and crystallization, are detected, confirming their amorphous natures. The T_g is adjustable in the range 8.8–54.1 °C based on the choice of the two monomers (**Figure S24**). This indicates the versatility of the ROAC system in designing APE materials with adjustable properties.

Terpolymerization of a cyclic anhydride and glycidylamine and another cyclic ether

Finally, we investigated terpolymerization of cyclic anhydrides, glycidylamines, and non-amino-functionalized epoxides to expand the range of accessible APE structures (**Scheme 3**). Terpolymerization was conducted using PA, BMGA, and BO as monomers, with *n*-butanol as the initiator, under the optimized conditions ([*t*-BuP$_1$]/[*n*-butanol]$_0$/[PA]$_0$/[BMGA]$_0$/[BO]$_0$ = 1/1/100/150/150, run 1 in **Table 5**). The initial mole fraction in the feed was f_{BMGA} = 0.5 (f_{BO} = 0.5). The simultaneous consumption of the three monomers is confirmed via ^{1}H NMR spectroscopy. The plots of the conv. values as functions of time reveal that BO consumption is faster than that of BMGA until the end of the reaction, suggesting that poly(PA-*alt*-BMGA)-*co*-poly(PA-*alt*-BO), with excess poly(PA-*alt*-BO) units, is obtained as a

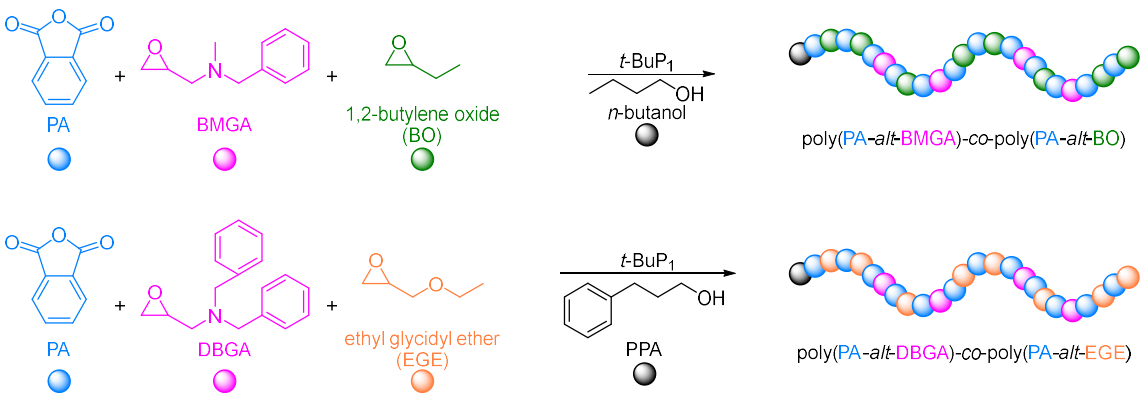

Scheme 3. Ring-opening terpolymerization of cyclic anhydride and glycidylamine with another epoxide.

Table 5. Ring-opening terpolymerization of PA, BMGA or DBGA, and BO or EGE [a]

run	Initiator (I)	$M_1/M_2/M_3$	[*t*-BuP$_1$]/[I]$_0$/[M$_1$]$_0$/[M$_2$]$_0$/[M$_3$]$_0$	time (h)	conv. (%) [b]	$M_{n,theo.}$ (g mol^{-1}) [c]	$M_{n,NMR}$ (g mol^{-1}) [b]	F_{M2} (mol.%) [b]	$M_{n,SEC}$ (g mol^{-1}) [d]	$Đ$ [d]
1	*n*-butanol	PA/BMGA/BO	1/1/100/150/150	2.0	PA = 92, BMGA = 28, BO = 46	24 000	6200	0.41	3120	2.23
2	*n*-butanol	PA/BMGA/BO	1/1/100/60/240	1.5	PA > 99, BMGA = 28, BO = 39	24 000	12 600	0.85	6050	1.75
3	PPA	PA/DBGA/EGE	1/1/100/150/150	5.0	PA = 84, DBGA = 24, EGE = 31	26 000	14 700	0.64	6350	1.39
4	PPA	PA/DBGA/EGE	1/1/100/60/240	3.0	PA > 99, DBGA = 8, EGE = 64	27 000	10 500	0.85	5580	1.38

[a] Polymerization conditions: temp., 80 °C; atmosphere, Ar; catalyst, *t*-BuP$_1$. [b] Determined via ^{1}H NMR spectroscopy in $CDCl_3$. [c] Calculated using (M.W. of initiator) + [PA]$_0$/[initiator]$_0$ × conv.$_{PA}$ × ((M.W. of PA + M.W. of glycidylamine) × (mol.% of glycidylamine) + (M.W. of PA + M.W. of epoxide) × (mol.% of epoxide)). [d] Determined via SEC in DMF containing 0.01 mol L^{-1} LiCl using a PSt. standard.

statistical copolyester (**Figure S25**). The ^{1}H NMR spectra of the obtained polymer together with the corresponding homopolymers (i.e. poly(PA-*alt*-BMGA) and poly(PA-*alt*-BO), see **Table S1**) demonstrated the appearance of the signals representing both poly(PA-*alt*-BMGA) (*a*–*g*) and poly(PA-*alt*-BO) units (*a*, *h*–*k*), confirming successful terpolymerization (**Figure S26**, left-hand panel). Based on the signal intensities *c* and *h*, the estimated mole fractions of BMGA and BO within the terpolymer are F_{BMGA} = 0.41 and F_{BO} = 0.59, respectively, which closely match the theoretical mole fractions calculated based on monomer conv. ($F_{calc.BMGA}$ = 0.37 and $F_{calc.BO}$ = 0.63). Although $Đ$ is slightly large (2.23), the SEC trace displays a unimodal elution peak (**Figure S26**, right-hand panel). Additionally, the covalent connection of the different blocks in the terpolyester was confirmed by the diffusion-ordered NMR (DOSY) analysis (**Figure S27**). Terpolymerization with an increased BO ratio ([PA]$_0$/[BMGA]$_0$/[BO]$_0$ = 100/60/240, f_{BMGA} = 0.2) also proceeds, yielding a terpolymer with F_{BMGA} = 0.15 (run 2 in **Table 5**). The ^{1}H NMR spectra of the terpolymers and the corresponding copolymers shown in **Figure S28** demonstrate the facile control based on f_{BMGA}.

Similarly, the terpolymerization of PA, DBGA, and ethyl glycidyl ether (EGE) was conducted in the presence of PPA and *t*-BuP$_1$ as the initiator and catalyst, respectively, with [*t*-BuP$_1$]/[PPA]$_0$/[PA]$_0$/[DBGA]$_0$/[EGE]$_0$ = 1/1/50/75/75 (f_{DBGA} = 0.5) affording poly(PA-*alt*-DBGA)-*co*-poly(PA-*alt*-EGE) with F_{BMGA} = 0.36 (**Figures S29–S31**). Moreover, F_{DBGA} can be adjusted by changing f_{DBGA} (**Figure S32**). Hence, the amino functional group contents of polyesters can be easily adjusted by incorporating an alkylene oxide or a glycidyl ether.

Conclusions

We established a novel pathway for use in synthesizing APEs based on the ROAC of cyclic anhydrides and glycidylamine. ROAC proceeded smoothly with alkali metal carboxylates and phosphazene bases as catalysts, but it also proceeded without a catalyst. Because of the controlled nature of this ROAC system, APEs with adjustable molecular weights and functional end groups could be produced. Moreover, the ROAC system enabled the syntheses of APEs with different main-chain structures by simply changing the combination of the two monomers. Considering the advantages of chain-growth polymerization and the wide monomer scope, the established ROAC system may accelerate the exploration of a novel class of APEs for use in different applications, e.g. as gene delivery carriers, antibacterial coatings, and biodegradable materials.

Author contributions

Ryota Suzuki: investigation, methodology, writing – original draft, visualization. **Tianle Gao:** investigation, methodology. **Ayaka Sumi:** investigation. **Takuya Yamamoto:** investigation, supervision. **Kenji Tajima:** investigation, supervision. **Feng Li:** investigation, supervision, writing – review and editing. **Takuya Isono:** investigation, supervision, writing – review and editing, funding acquisition. **Toshifumi Satoh:** conceptualization, writing – review and editing, supervision, project administration, funding acquisition.

Conflicts of interest

There are no conflicts to declare

Data availability

The data supporting this article have been included as part of the ESI.†

Acknowledgments

This work was financially supported by the Japan Society for the Promotion of Science Grant-in-Aid for Challenging Research (Grant 22K19907), Grant-in-Aid for Scientific Research (A) (Grant 24H00766), Grant-in-Aid for JSPS Research Fellows, the Frontier Chemistry Center (Hokkaido University),

the Photo-Excitonic Project (Hokkaido University), the Creative Research Institution (CRIS, Hokkaido University), the List Sustainable Digital Transformation Catalyst Collaboration Research Platform (List-PF, Hokkaido University), and the Project of Junior Scientist Promotion (Hokkaido University). R. Suzuki gratefully acknowledges the JSPS Fellowship for Young Scientists.

Notes and references

1 Y. Nagasaki, *Chem. Lett.*, 2008, **37**, 564–569.
2 J. Peng, F. Liu, F. Feng, X. Feng and J. Cui, *ACS Sustainable Chem. Eng.,* 2023, **11**, 13805–13811.
3 M. Kim, J. Park, K. M. Lee, E. Shin, S. Park, J. Lee, C. Lim, S. K. Kwak, D. W. Lee and B.-S. Kim, *J. Am. Chem. Soc.*, 2022, **144**, 6261–6269.
4 C. Taplan, M. Guerre and F. E. D. Du Prez, *J. Am. Chem. Soc.*, 2021, **143**, 9140–9150.
5 F. Schacher, M. Ulbricht and A. H. E. Müller, *Adv. Funct. Mater.,* 2009, **19**, 1040–1045.
6 P. Stenström, E. Hjorth, Y. Zhang, O. C. J. Andrén, S. Guette-Marquet, M. Schultzberg and M. Malkoch, M. *Biomacromolecules*, 2017, **18**, 4323–4330.
7 J. Ma, M. Shao, N. Ma, J. Liu, Y. Tang, W. Qu and W. Zhang, *ACS Appl. Polym. Mater.,* 2023, **5**, 3643–3652.
8 Y. Yan, H. Xiong, X. Zhang, Q. Cheng and D. J. Siegwart, *Biomacromolecules*, 2017, **18**, 4307–4315.
9 J. Hao, P. Kos, K. Zhou, J. B. Miller, L. Xue, Y. Yan, H. Xiong, S. Elkassih and D. J. Siegwart, *J. Am. Chem. Soc.*, 2015, **137**, 9206–9209.
10 O. Lunov, T. Syrovets, C. Loos, G. U. Nienhaus, V. Mailänder, K. Landfester, M. Rouis and T. Simmet, *ACS Nano*, 2011, **5**, 9648–9657.
11 Z. Shi, F. Guo, Y. Li and Z. Hou, *J. Polym. Sci. Part A: Polym. Chem.*, 2015, **53**, 5–9.
12 J. Blankenburg, M. Wagner and H. Frey, *Macromolecules*, 2017, **50**, 8885–8893.
13 V. S. Reuss, B. Obermeier, C. Dingels and H. *N*. Frey, *Macromolecules*, 2012, **45**, 4581–4589.
14 J. Lee, A. J. McGrath, C. J. Hawker and B.-S. Kim, *ACS Macro Lett.*, 2016, **5**, 1391–1396.
15 P. Verkoyen and H. Frey, *Polym. Chem.*, 2020, **11**, 3940–3950.
16 M. M. A. Abd Elwakil, R. Suzuki, A. M. Khalifa, R. M. Elshami, T. Isono, Y. H. A. Elewa, Y. Sato, T. Nakamura, T. Satoh and H. Harashima, *Adv. Funct. Materials*, 2023, **33**, 2303795.
17 T. Isono, S. Asai, Y. Satoh, T. Takaoka, K. Tajima, T. Kakuchi and T. Satoh, *Macromolecules*, 2015, **48**, 3217–3229.
18 C.-Y. Won, C.-C. Chu and J. D. Lee, *Polymer*, 1998, **39**, 6677–6681.
19 E. A. Chamsaz, S. Mankoci, H. A. Barton and A. Joy, *ACS Appl. Mater. Interfaces*, 2017, **9**, 6704–6711.
20 M. O. Arıcan, S. Erdoğan and O. Mert, *Macromolecules*, 2018, **51**, 2817–2830.
21 M. Deng, J. Wu, C. A. Reinhart-King and C.-C. Chu, *Biomacromolecules*, 2009, **10**, 3037–3047.
22 Y. Bernhard, J. F. R. V. Van Guyse, M. Purino and R. Hoogenboom, *Eur. Polym. J.*, 2023, **192**, 112077.
23 A. Bentolila, I. Vlodavsky, R. Ishai-Michaeli, O. Kovalchuk, C. Haloun and A. J. Domb, *J. Med. Chem.,* 2000, **43**, 2591–2600.
24 A. K. Yamala, V. Nadella, Y. Mastai, H. Prakash and P. Paik, *Nanoscale*, 2017, **9**, 14006–14014.
25 J. Hao, S. Elkassih and D. J. Siegwart, *Synlett*, 2016, **27**, 2285–2292.
26 Y. Wei, X. Li, H. Yuan, Y. Qi and Y. Huang, *Polymer*, 2024, **296**, 126820.
27 D. A. Barrera, E. Zylstra, P. T. Lansbury Jr and R. Langer, *J. Am. Chem. Soc.*, 1993, **115**, 11010–11011.
28 Y.-B. Lim, C.-H. Kim, K. Kim, S. W. Kim and J.-S. Park, *J. Am. Chem. Soc.*, 2000, **122**, 6524–6525.
29 W. W. Gerhardt, D. E. Noga, K. I. Hardcastle, A. J. García, D. M. Collard and M. Weck, *Biomacromolecules,* 2006, **7**, 1735–1742.
30 X. Chen, H. Lai, C. Xiao, H. Tian, X. Chen, Y. Tao and X. Wang, *Polym. Chem.*, 2014, **5**, 6495–6502.
31 T. R. Blake and R. M. Waymouth, *J. Am. Chem. Soc.*, 2014, **136**, 9252–9255.
32 C.-K. Chen, C. H. Jones, P. Mistriotis, Y. Yu, X. Ma, A. Ravikrishnan, M. Jiang, S. T. Andreadis, B. A. Pfeifer and C. Cheng, *Biomaterials*, 2013, **34**, 9688–9699.
33 Z. Zhang, L. Yin, Y. Xu, R. Tong, Y. Lu, J. Ren and J. Cheng, *Biomacromolecules*, 2012, **13**, 3456–3462.
34 Z.-Y. Li, X. Zhang, Y.-L. Qian, F.-S. Du and Z.-C. Li, *J. Mater. Chem. B*, 2024, **12**, 1569–1578.
35 S. Blanquer, J. Tailhades, V. Darcos, M. Amblard, J. Martinez, B. Nottelet and J. Coudane, *J. Polym. Sci. A Polym. Chem.*, 2010, **48**, 5891–5898.
36 H. Han, J. Zhu, F.-F. Zhang, F.-X. Li, X.-L. Wang, J.-Y. Yu, X.-H. Qin and D.-Q. Wu, *Biomater. Sci.*, 2019, **7**, 5404–5413.
37 Y. Liu, D. Wu, Y. Ma, G. Tang, S. Wang, C. He, T. Chung and S. Goh, *Chem. Commun. (Camb)*, 2003, **20**, 2630–2631.
38 J. C. Kaczmarek, A. K. Patel, K. J. Kauffman, O. S. Fenton, M. J. Webber, M. W. Heartlein, F. DeRosa and D. G. Anderson, *Angew. Chem. Int Ed Engl*, 2016, **55**, 13808–13812.
39 U. S. Gunay, M. Cetin, O. Daglar, G. Hizal, U. Tunca and H. Durmaz, *Polym. Chem.*, 2018, **9**, 3037–3054.
40 T. Tang and A. Takasu, *RSC Adv.*, 2015, **5**, 819–829.
41 R. Xie, G.-W. Yang, Y.-Y. Zhang, C. Lu, W.Li, J. Wang and G.-P. Wu, *Polym. Chem.*, **2024**, *15*, 412–421.
42 J. Herzberger, D. Kurzbach, M. Werre, K. Fischer, D. Hinderberger and H. Frey, *Macromolecules*, 2014, **47**, 7679–7690.
43 V. S. Reuss, M. Werre and H. Frey, *Macromol. Rapid Commun.*, 2012, **33**, 1556–1561.
44 B. Obermeier, F. Wurm and H. Frey, *Macromolecules*, 2010, **43**, 2244–2251.
45 R. Suzuki, X. Xia, T. Gao, T. Yamamoto, K. Tajima, T. Isono and T. Satoh, *Polym. Chem.*, 2022, **13**, 5469–5477.
46 X. Xia, R. Suzuki, K. Takojima, D.-H. Jiang, T. Isono and T. Satoh, *ACS Catal.*, 2021, **11**, 5999–6009.
47 X. Xia, R. Suzuki, T. Gao, T. Isono and T. Satoh, *Nat. Commun.*, 2022, **13**, 163.
48 X. Xia, T. Gao, F. Li, R. Suzuki, T. Isono and T. Satoh, *J. Am. Chem. Soc.*, 2022, **144**, 17905–17915.
49 X. Xia, T. Gao, F. Li, R. Suzuki, T. Isono and T. Satoh, *Macromolecules*, 2023, **56**, 92–103.
50 F. Li, R. Suzuki, T. Gao, X. Xia, T. Isono and T. Satoh, *Bull. Chem. Soc. Jpn*, 2023, **96**, 1003–1018.
51 I. Ota, R. Suzuki, Y. Mizukami, X. Xia, K. Tajima, T. Yamamoto, F. Li, T. Isono and T. Satoh, *Macromolecules*, 2024, **57**, 3741–3750.
52 A. Kummari, S. Pappuru and D. Chakraborty, *Polym. Chem.*, **2018**, *9*, 4052–4062.
53 K. Bester, A. Bukowska, B. Myśliwiec, K. Hus, D. Tomczyk, P. Urbaniak and W. Bukowski, *Polym. Chem.*, **2018**, *9*, 2147–2156.
54 D. Kurzbach, V. S. Wilms, H. Frey and D. Hinderberger, *ACS Macro Lett.*, 2013, **2**, 128–131.